

CO₂ has hardly any effect on the surface temperature

Joseph Reynen

Port Marina Baie des Anges

Le Ducal U111

06270 Villeneuve-Loubet, France

jwreynen@aol.co

September 2015

updated November 2015

Introduction

In earlier papers [1,2] the author has described models to analyze the evacuation of heat from the surface of the planet, representing the atmosphere by semi-transparent grids. In those papers the one-stream heat flow formulation is used without the non-physical back-radiation, from cold to warm, and thereby non-physical huge LW surface radiation. IPCC (International Panel for Climate Change) authors have adopted the Schwarzschild procedure, en vogue in astronomy, with a two-stream formulation. Unfortunately IPCC authors interpret radiation always as radiation of heat, with the non-physical back radiation of heat. The astronomer Ferenc Miskolczi (FM) uses the two-stream formulation. But FM speaks about “Global average radiative equilibrium structure with constant optical height”, and not about back-radiation of heat [3].

In [1] the author has used the one-stream stack model to carry out a sensitivity analysis of doubling CO₂ concentration. For a model of 10 km height, a surface temperature increase $\delta T_s = 0.03$ K was obtained. In this paper the sensitivity analysis is repeated for a model with an height of 30 km, in order to take into account the traces of CO₂ at those heights. The sensitivity from zero to 400 ppm is 0.04 K or $1e-4$ K/ppmCO₂.

Two-stream formulation authors do not agree on the CO₂ sensitivity with each other.

FM [3] uses the line-by-line computer program HARTCODE and speaks about a to be neglected effect of CO₂, although weather balloons measurements show, according to FM, a decrease in average water vapor for an increase in CO₂ concentration.

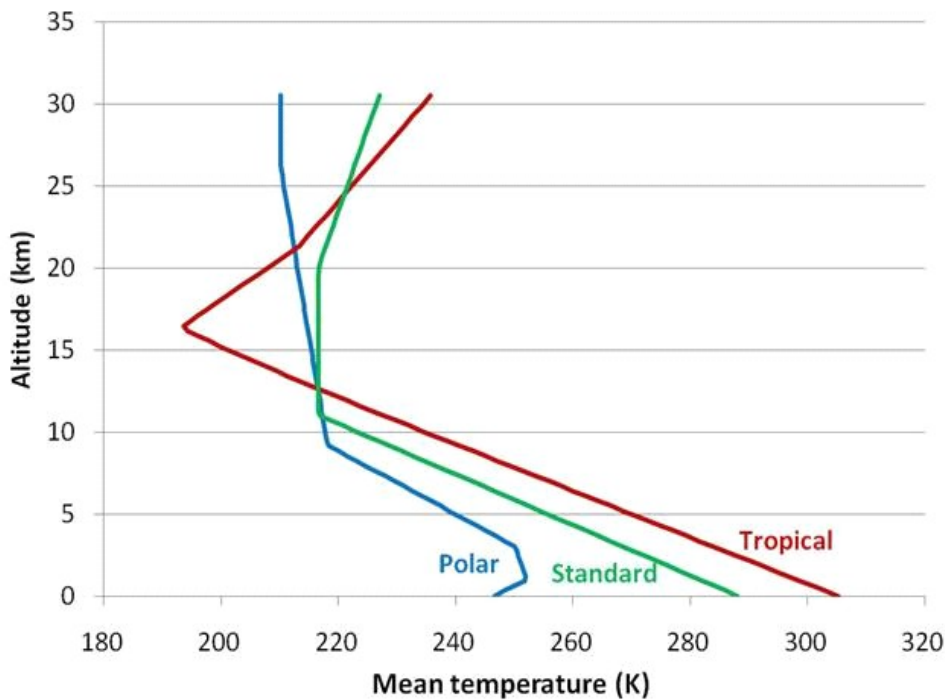
But IPCC authors give what they call CO₂-forcing or $\delta OLR_{CO_2} = -3.5$ W/m², obtained from computer programs where the effect of CO₂ is obtained by artificially broadening the CO₂ line in the spectrum [8]. With the variation of OLR due to surface temperature $dOLR/dT_s = 3.4$ W/m²/K, the value for surface temperature increase becomes a factor 25 too big. IPCC: $\delta T_s = -\delta OLR_{CO_2}/(dOLR/dT_s) = 3.5/3.4 = 1.0$ K.

The stack model does not confirm the suggestion of Kyoji Kimoto [9] that a variation of the lapse rate could be an alternative to the fixed lapse rate sensitivity analysis.

Sensitivity Analysis

The stack model is based on the measured temperature distribution in the troposphere, defined by gravitation and the specific heat of air, giving rise to lapse rates: the dry adiabatic lapse rate, $DALR = -g/c_p = -9.8 \text{ K/km}$, and the measured environmental lapse rate, $ELR = -6.5 \text{ K/km}$, depending also on the latent heat of wet air and convection. In **figure 1** the temperature profiles for three different climate zones are given.

Figure 1 from the Public Domain Aeronautical Software [4]



We observe the parallel lines in the temperature profiles in the troposphere for the various zones, with a slope equal to the environmental lapse rate, $ELR = -6.5 \text{ K/km}$. The slope remains constant, since it is defined by gravity and the specific heat of air and the latent heat. Only the surface temperature varies, due to the variation of sun power, higher in the tropical zone and lower in the polar zone: an average value of $T_s = 288 \text{ K}$ for the standard profile with an OLR of 240 W/m^2 .

For the various climate zones different surface temperatures are established because the evacuation mechanisms of heat, - radiation but mainly convection - , from the surface to outer-space, depend on the temperature distribution *i.e* $OLR = 240 \text{ W/m}^2$ for the standard atmosphere with $ELR = -6.5 \text{ K/km}$ with surface temperature $T_s = 288 \text{ K}$.

The basic relations of the stack model are written in matrix form, (**bold** symbols stand

for matrices or vectors), representing the heat balances by LW radiation between the surface of the planet and lower grids and for grids at higher height to outer-space [1].

$$\mathbf{K} * \boldsymbol{\theta} = \mathbf{rhs} \quad (1)$$

K : System matrix of order NxN, to be modified by boundary conditions.

It is generated for water vapor and for CO₂, respectively **Kh2o** and **Kco2**

θ : Vector of unknowns, W/m², of order N, typical 60 for a height of 30 km.

The variables represent temperature, $\theta_i = \sigma T_i^4$

rhs : Right hand side vector of fluxes q , W/m², into the system, of order N

To solve the system of equations (1) , boundary conditions are needed.

At the surface of the planet at node 1: $T_1 = T_s$, or $\theta_1 = \sigma T_s^4$.

For outer-space at node N: $\theta_N = 0$.

For a known matrix **K** and known right hand side vector **rhs**, the relation (1) gives the possibility to calculate the temperature distribution **θ** in the atmosphere.

Examples are given in [2] for a **rhs=0**, so to speak a stack on the moon, or as if the stack in the atmosphere of the Earth, representing the IR-active trace gases, were isolated from the bulk of the atmosphere, 99% O₂ and N₂.

But for a stack on the real planet Earth the loading vector **rhs** should contain the effect of heat transport by convection, which is not obvious.

However with known measured temperature profiles of **figures 1**, mainly defined by gravity, we look to the reversed equations:

$$\mathbf{qh2o} = \mathbf{Kh2o} * \boldsymbol{\theta} \quad \text{and} \quad \mathbf{qco2} = \mathbf{Kco2} * \boldsymbol{\theta} \quad (2)$$

Kh2o , **Kco2** : system matrices of order NxN (in the sensitivity analysis N=60).

They represent the contributions of water vapor H₂O and of CO₂.

θ : vector of N known temperature parameters.

qh2o , **qco2** : vectors of to be calculated fluxes, into the system, of order N, W/m².

The calculated vectors **qh2o** and **qco2** in (2) consist each of N components:

qh2o(1) , qco2(1) : LW surface fluxes

qh2o(N) , qco2(N) : - OLRh2o , - OLRco2 , outgoing LW radiations

The remaining terms, $i=2:N-1$, represent heat input at the various axial stations in a column of air due to mechanisms other than LW radiation: convection of latent and sensible heat and absorption by the atmosphere of incoming SW radiation.

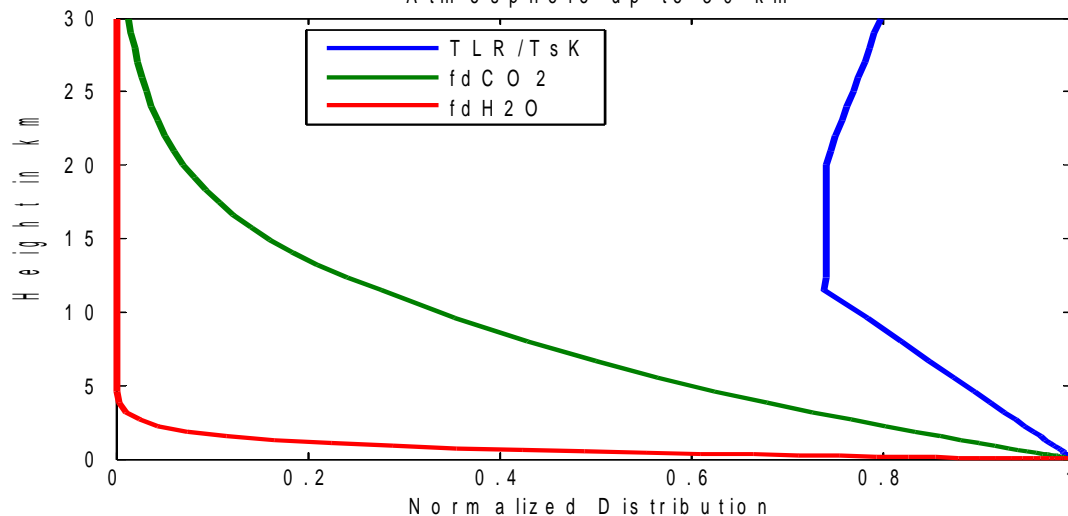
The radiation matrices \mathbf{K}_{H_2O} , \mathbf{K}_{CO_2} depend on the distribution of the traces of IR-active gases, such as water vapor H_2O and CO_2 .

The distribution of water vapor H_2O and CO_2 have been discussed in detail in [1].

The temperature in **figure 2** correspond to the standard atmosphere of **figure 1**.

Figure 2

fig 5.3 Normalized Temperature, water vapor form $m = 7$ and CO_2 distribution Atmosphere up to 30 km



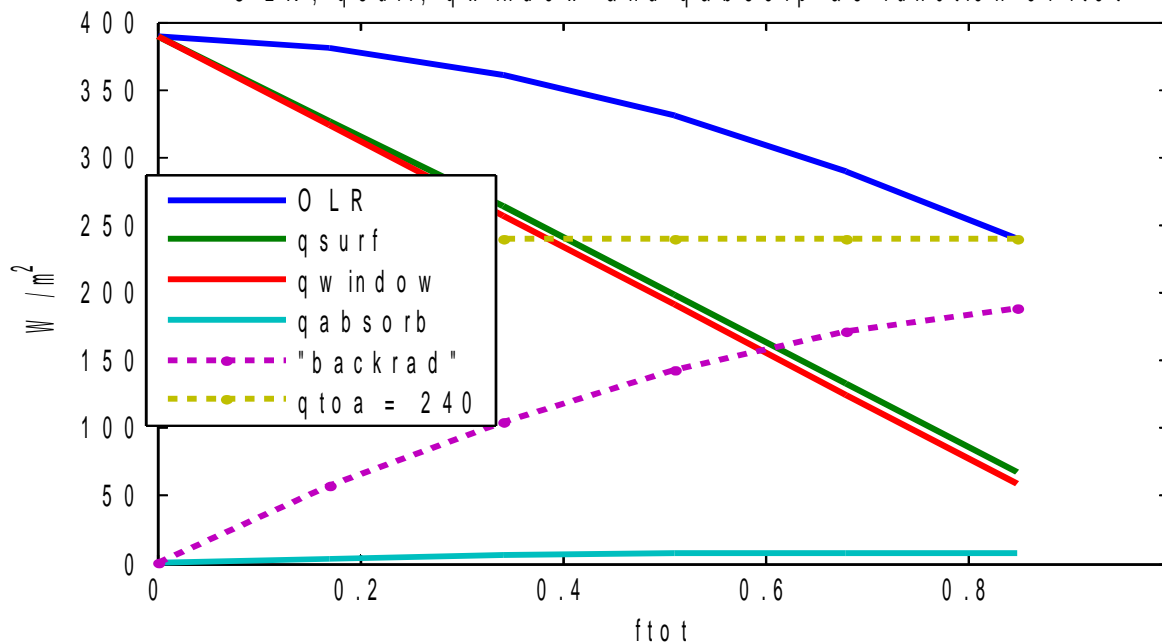
The main results of the stack-model, $q=K*\theta$, are represented in **figure 3**.

Figure 3

fig 5.1 Main result of stack model

$w = 1$ Planck = 4 nodes = 60 m = 7 height = 30 km LR = -6.5 K/km TsK = 2
 "backrad" is not backradiation of heat

O L R, q_{surf} , q_{window} and q_{absorb} as function of $ftot$



The equilibrium point is for $f_{tot} = f_{tot2o} + f_{totco2} = 0.849$:

OLR=240 , LW $q_{surf} = 67$ of which $q_{window} = 59$ and $q_{absorb} = 8$.

In **Appendix 1** these results are compared in detail with those of Ferenc Miskolczi [3].

The results of **figure 3** are for a surface temperature $T_sK = 288$.

The variations of the surface temperature T_sK between climate zones and thereby variation of OLR, surface flux and window flux are given in **figure 4**.

Figure 4

fig 2.7 Steady state solutions for various atmospheric and surface temperature
 Atmospheric temperature according to lapse rate $LR = -6.5$
 Starting from surface temperature (x-axis)

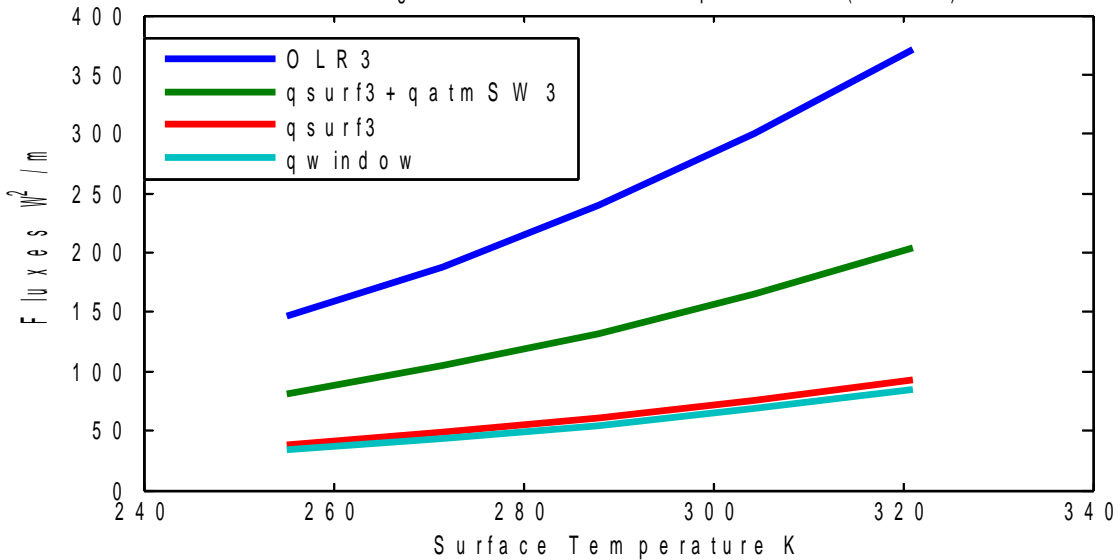
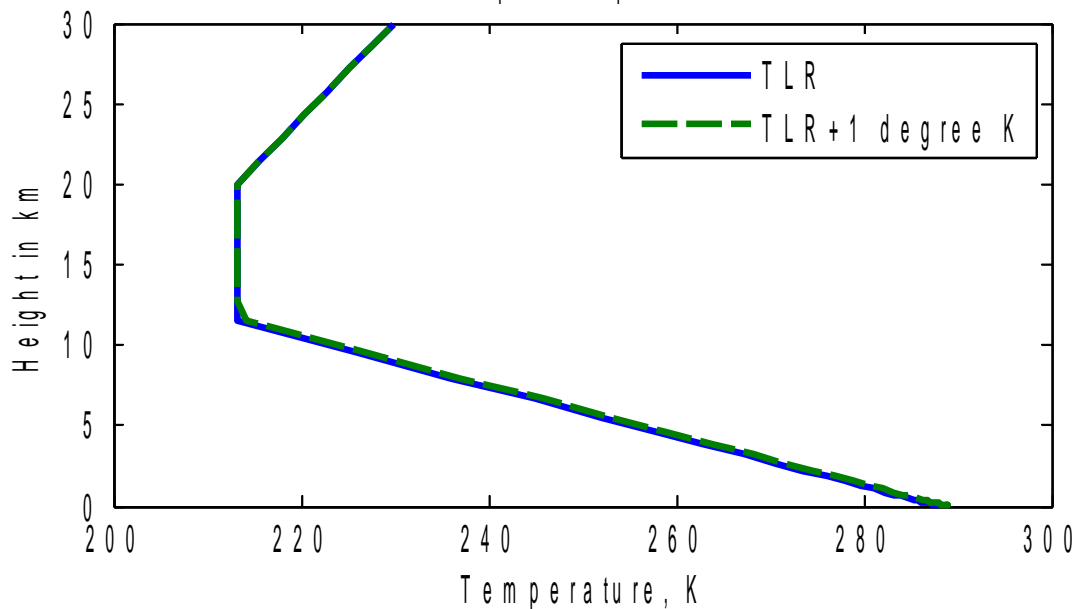


Figure 5

fig 5.1 Temperature distribution in atmosphere
 Atmosphere up to 30 km



The variations of temperature and OLR with variations of CO₂ concentrations are much smaller than the differences between the climate zones depicted in **figures 1 and 3**. IPCC authors claim 1.0 K for doubling the CO₂ concentration from 400 to 800 ppm. The translation of the temperature profile is hardly visible as can be seen from **figure 5** for a $\delta T_s = 1\text{K}$. We will show that the variation of surface temperature for CO₂ doubling is even much smaller: $\delta T_s = 0.04\text{ K}$.

For the sensitivity analysis we have to look in detail to the system equations **(2)** and doing some algebra on them:

$$\mathbf{qh2o} = \mathbf{Kh2o} * \theta \quad \text{and} \quad \mathbf{qco2} = \mathbf{Kco2} * \theta \quad \text{(2bis)}$$

The outgoing long wave radiations OLR_{h2o} and OLR_{co2} are represented by the components $-\mathbf{qh2o}(N)$ and $-\mathbf{qco2}(N)$.

With **knodsco2** and **knodsh2o** representing the rows $N = \text{nods}$ ($=60$) of respectively **Kco2** and **Kh2o**, the individual, standalone, outgoing LW radiations become:

$$\text{OLRco2} = - \mathbf{knodsco2} * \theta \quad \text{and} \quad \text{OLRh2o} = - \mathbf{knodsh2o} * \theta \quad \text{(3)}$$

For concentrations f_{otco2} and f_{oth2o} of the IR-active gases zero, and when dealt with separately OLR_{co2} and OLR_{h2o} are both equal to the surface flux $\epsilon \sigma T_s^4 = \epsilon \theta(1)$. The individual forcings from CO₂ and H₂O become, respectively

$$\Delta \text{OLRco2} = \epsilon \theta(1) - \text{OLRco2} = \epsilon \theta(1) + \mathbf{knodsco2} * \theta \quad \text{(4)}$$

$$\Delta \text{OLRh2o} = \epsilon \theta(1) - \text{OLRh2o} = \epsilon \theta(1) + \mathbf{knodsh2o} * \theta$$

The OLR from simultaneously present CO₂ and H₂O concentrations becomes:

$$\begin{aligned} \text{OLR} &= \epsilon \theta(1) - \Delta \text{OLRco2} - \Delta \text{OLRh2o} \\ &= - \epsilon \theta(1) - (\mathbf{knodsco2} + \mathbf{knodsh2o}) * \theta \end{aligned} \quad \text{(5)}$$

In **(5)** we have defined the resulting outgoing LW radiation of the components defined by the system equation of the two contributions from **(3)**. The relation becomes easier to write down and to program, when the scalar surface emission ϵ is converted to a row vector $\boldsymbol{\epsilon}$ with only the first component not equal to zero: $\boldsymbol{\epsilon} = [\epsilon, 0, 0, \dots, 0]$. The combined OLR becomes:

$$\begin{aligned} \text{OLR} &= -(\boldsymbol{\epsilon} + \mathbf{knodsco2} + \mathbf{knodsh2o}) * \theta \\ &= -(\mathbf{knodsco2} + (\boldsymbol{\epsilon} + \mathbf{knodsh2o})) * \theta \end{aligned} \quad \text{(6)}$$

Taking the constant ϵ row vector together with the **knodsh2o** row vector has an advantage in the variation procedure of CO₂ concentration with a constant H₂O concentration.

With the chain rule:

$$\delta\text{OLR} = -\delta(\mathbf{knodsco2}) * \boldsymbol{\theta} - (\mathbf{knodsco2} + (\epsilon + \mathbf{knodsh2o})) * \delta\boldsymbol{\theta} \quad (7)$$

We see that the OLR variation depends on the concentration of IR-active gases CO₂ and H₂O through the 2 times 60 components of **knodsco2** and **knodsh2o** and the 60 temperature parameters through the 60 components of $\boldsymbol{\theta}$ and the variation thereof.

In a sensitivity analysis OLR remains constant, an increase in one term is compensated by a decrease in the other term, in such a way that $\delta\text{OLR}=0$.

It is assumed that **knodsh2o** does not change with a variation of CO₂, although Ferenc Miskolczi [3] has observed, by means of weather balloons, that water vapor concentration decreases for an increase in CO₂ concentration.

The first term in the right hand side of (7) becomes:

$$\delta(\mathbf{knodsco2}) * \boldsymbol{\theta} = -\mathbf{knodsco2} * \boldsymbol{\theta} - \sigma T_s^4 = \delta\text{OLR}_{\text{co2}} \quad (8)$$

It is the variation of OLR from zero to the present value of 400 ppm which is the same as from the present variation to 800 ppm.

We see that (8) is the equivalent of (4).

The variation $\delta\boldsymbol{\theta}$ is calculated from:

$$\begin{aligned} \delta\boldsymbol{\theta} &= \delta(\sigma \mathbf{T}^4) = 4 \sigma \mathbf{T}^3 \delta(T_s + \text{ELR} * \mathbf{z}) \\ &= 4\sigma \mathbf{T}^3 (\delta T_s + \text{ELR} * \mathbf{z}) = \boldsymbol{\Psi} \delta T_s + \boldsymbol{\Phi} \delta \text{ELR} \end{aligned} \quad (9)$$

$$\boldsymbol{\theta} = [\theta_1, \theta_2, \dots, \theta_N]' = \sigma [T_1^4, T_2^4, \dots, T_N^4]'$$

$$\boldsymbol{\Psi} = [\Psi_1, \Psi_2, \dots, \Psi_N]' = 4 \sigma [T_1^3, T_2^3, \dots, T_N^3]'$$

$$\boldsymbol{\Phi} = [\Phi_1, \Phi_2, \dots, \Phi_N]' = 4 \sigma [z_1 T_1^3, z_2 T_2^3, \dots, z_N T_N^3]'$$

The apostrophe means that the column vectors are written as row vectors: transpose.

In (9) not only the variation of the surface temperature is taken into account but also an eventual variation of the lapse rate ELR.

Influence of the surface temperature

The second term in the right hand side of (7) for a variation δT_s becomes:

$$(\text{knodsco2} + (\epsilon + \text{knodsh2o})) \cdot \Psi \delta T_s = (d\text{OLR}/dT_s) \delta T_s \quad (10)$$

The derivative $d\text{OLR}/dT_s = (\text{knodsco2} + (\epsilon + \text{knodsh2o})) \cdot \Psi$ represents the slope of OLR in **figure 4** at the point $T_s=288$ K.

For the equilibrium point, $f_{\text{tot}} = 0.849$ and $\text{OLR} = 240$:

$$d\text{OLR}/dT_s = 3.4 \text{ W/m}^2/\text{K} \quad (11)$$

Note: The derivative of OLR with respect to surface temperature T_s is sometimes approached by $d\text{OLR}/dT_s = d(\sigma T_s^4)/dT_s = 4 \sigma T_s^3 = 5.42 \text{ W/m}^2/\text{K}$. The value $3.4 \text{ W/m}^2/\text{K}$ of (11) takes into account temperature and distribution of IR-active gases, CO_2 and H_2O , in the atmosphere by (9).

With (8) and (11) the variation of the surface temperature becomes:

$$\delta T_s = -\delta\text{OLR}_{\text{co2}} / (d\text{OLR}/dT_s) \quad (12)$$

We analyze values of the present f_{totco2} between 0.1% and 3% of the total present $f_{\text{tot}} = f_{\text{toH}_2\text{O}} + f_{\text{totco2}}$.

In **table 1** are given for different ratios $f_{\text{totco2}}/f_{\text{tot}}$ the results of the sensitivity analysis of the stack model:

Table 1 CO_2 sensitivity as function of assumed ratio of effect of 0.04% CO_2 versus 4% H_2O

$f_{\text{totco2}}/f_{\text{tot}} \%$	$\delta\text{OLR}_{\text{co2}} \text{ W/m}^2$	$\delta T_s_{2x\text{CO}_2} \text{ K}$	$\delta T_s \text{ K/ppmCO}_2$
0.1	-0.13629	0.04	1 e-4
1	-1.3717	0.4	10 e-4
2	-2.763	0.83	21 e-4
2.5	-3.47	1.04	26 e-4

In **table 1** is given a great gamma of entries for $f_{\text{totco2}}/f_{\text{tot}}$ from 0.1% to 2.5%.

The reason is that we want to draw the attention on the fact that the stack model is nearly completely linear! Indeed, **table 1** does not show the strange IPCC logarithmic dependence on the magnitude of the concentration of traces of IR-active gas CO_2 , probably a result of the artificial broadening of the CO_2 line in MODTRAN. [7]

Since Ferenc Miskolczi with the line-by-line HARTCODE analyses of weather balloon measurements, reports a negligible effect of CO_2 , the lower value obtained by the contribution 0.1% of f_{tot} is retained: CO_2 -sensitivity $\delta T_s = 1 \text{ e-4 K/ppmCO}_2$

Influence of the lapse rate ELR

In a recent paper by Kyoji Kimoto [9] , it was suggested that the variation of the lapse rate ELR with the CO₂ concentration could be an alternative to the variation of the surface temperature and a fixed lapse rate.

The second term in the right hand side of (7) for a variation δELR becomes:

$$(\mathbf{knodscO2} + (\epsilon + \mathbf{knodsh2O})) * \Phi \delta ELR = (dOLR/dELR) \delta ELR \quad (13)$$

With (8) and (13) the variation of the surface temperature becomes:

$$\delta ELR = - \delta OLR_{CO2} / (dOLR/dELR) \quad (14)$$

In table 2 the numerical results are given for $dOLR/dELR$, δELR , δT_{toa} .

Table 2 ELR sensitivity as function of assumed present effect of CO₂ versus present effect of H₂O

$$ELR = - 6.5 \text{K/km}, z_{toa} = 11 \text{km}, \delta T_{toa} = \delta ELR * z_{toa}$$

% ftotco2/ftot	W/m ² δOLR_{CO2}	W/m ² /(K/km) $dOLR/dELR$	K/km δELR	K/km $ELR + \delta ELR$	K δT_{toa}	K δT_s
0.1	-0.13629	2.39	0.057	-6.44	0.63	0
1	-1.3717	2.49	0.44	-6.06	4.84	0
2	-2.763	2.67	1.03	-5.47	11.37	0
2.5	-3.47	2.74	1.26	-5.24	13.88	0

We see that the numerical results of the stack model do not confirm the suggestion of Kyoji Kimoto [9], the necessary variation of the lapse rate and temperature variation at TOA are far too big. The standard atmosphere for the different climate zones, depicted in **figure 1**, shows for the variation of the OLR from tropical to polar zones a nearly constant lapse rate $ELR = - 6.5 \text{ K/km}$.

Conclusion

The finite element stack model based on an one-stream formulation of heat radiation from warm to cold gives clear answers for both the global heat balance as well as the sensitivity of doubling the CO₂ concentration.

In the global balances there is no place for the non-physical back-radiation of heat and thereby huge LW surface radiation, to be absorbed by the atmosphere in order to be radiated back, according to the two-stream heat flow formulation.

The evacuation of heat is mainly by convection from the surface of the planet to higher layers and only from thereon by radiation to outer-space.

The stack model gives an increase of 0.04 K for doubling of the present 0.04 % CO₂ in the atmosphere by assuming that the effect of CO₂, is 0.1% of the effect of 4% water vapor in the atmosphere. The total absorption coefficient of the atmosphere for OLR =240 is $f_{tot} = 0.849$ and the contribution of CO₂ is $f_{totCO_2} = 0.000849$. The result is $\delta T_{S_{2 \times CO_2}} = 0.04$ K or $\delta T_s = 1 \text{ e-4 K/ppmCO}_2$.

Ferenc Miskolczi claims a negligible CO₂ sensitivity, also due to the measured decrease in water vapor for an increase in CO₂. FM uses the line-by-line HARDCODE computer program, avoiding the artificial broadening of the CO₂ line in the spectrum of programs like MODTRAN and HITRAN. IPCC authors give as CO₂-forcing -3.5 W/m², which corresponds to a sensitivity for CO₂ doubling: $\delta T_{S_{2 \times CO_2}} = 1.0$ K

A factor 25 higher as compared to the results of the stack model.

The reason of this difference is the artificial broadening of the CO₂ spectrum line in the software used by IPCC authors.

Acknowledgment

The author wants to thank in particular [Claes Johnson](#) who inspired him to write this paper. The author interpreted his ideas by writing Stefan-Boltzmann always for a **pair** of surfaces: it opens the concept of standing waves.

The efficient help of [Hans Schreuder](#) to edit and to host my papers on his site and give them a broader distribution is appreciated as well as the suggestions by the peer reviewers which Hans has called upon.

Thanks also to John O'Sullivan at [Principia Scientific International](#) for the publication of this paper.

References

- [1] http://principia-scientific.org/publications/PROM/PROM_REYNEN_Finite_Element.pdf
- [2] <http://www.tech-know-group.com/papers/vacuum.pdf>
- [3] <http://www.seipub.org/des/Download.aspx?ID=21810>
- [4] <http://www.pdas.com/hotcold.html>
- [5] <http://www.tech-know-group.com/papers/Reynen-MATLAB-listing.pdf>
- [6] <http://claesjohnson.blogspot.fr/>
http://edberry.com/blog/authors-climate/kyoji-kimoto/basic-global-warming-hypothesis-is-wrong/?awt_l=KQtMI&awt_m=3heA_pa1ka7WuNE
- [7] <http://claesjohnson.blogspot.fr/search/label/IPCC%20Trick>
- [8] http://folk.uio.no/gunnarmy/paper/myhre_grl98.pdf
- [9] http://edberry.com/blog/authors-climate/kyoji-kimoto/basic-global-warming-hypothesis-is-wrong/?awt_l=KQtMI&awt_m=3heA_pa1ka7WuNE

Appendix 1

Comparison of stack model and Miskolczi model

Ferenc Miskolczi, FM, [3] has presented a global average energy budget.

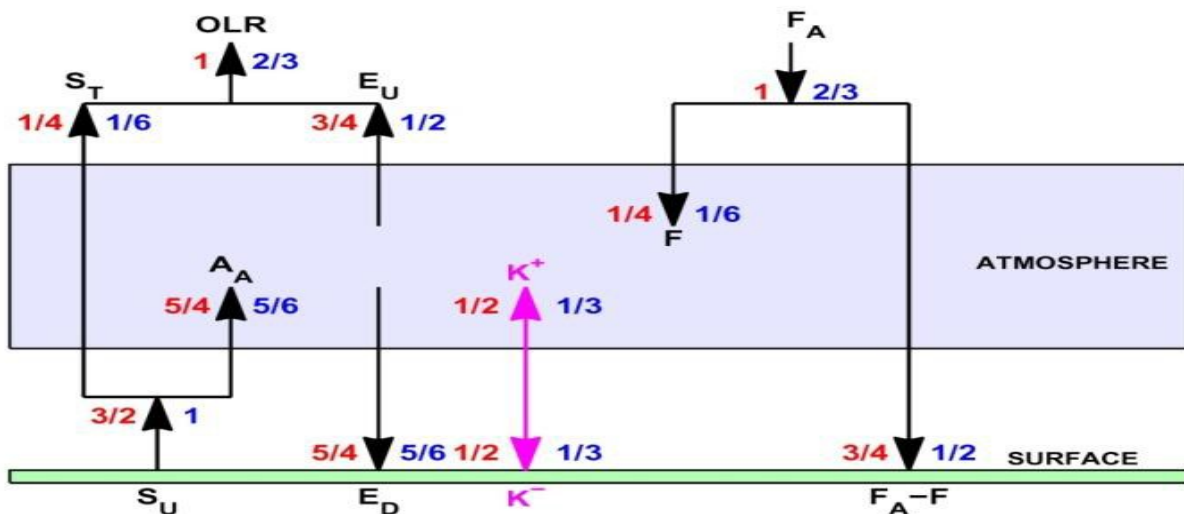
It is reproduced here as **figure A1**, a copy of **figure 24** in [3].

FM uses the two-stream formulation of LW radiation and comes up with huge absorption in the atmosphere, huge LW back-radiation, huge LW surface flux! Typical non-physical two-stream issues, like IPCC authors.

Figure A1 copied from figure 24 of [3].

Global average radiative equilibrium structure with constant τ_A

$$T_A = S_T / S_U = 1 / 6, \tau_A = 1.792 \quad g = 0.3240 \sim 1/3$$



In **figure A1** the red numbers correspond to *normalized value* $OLR=1$ and the blue figures to $SU=1$.

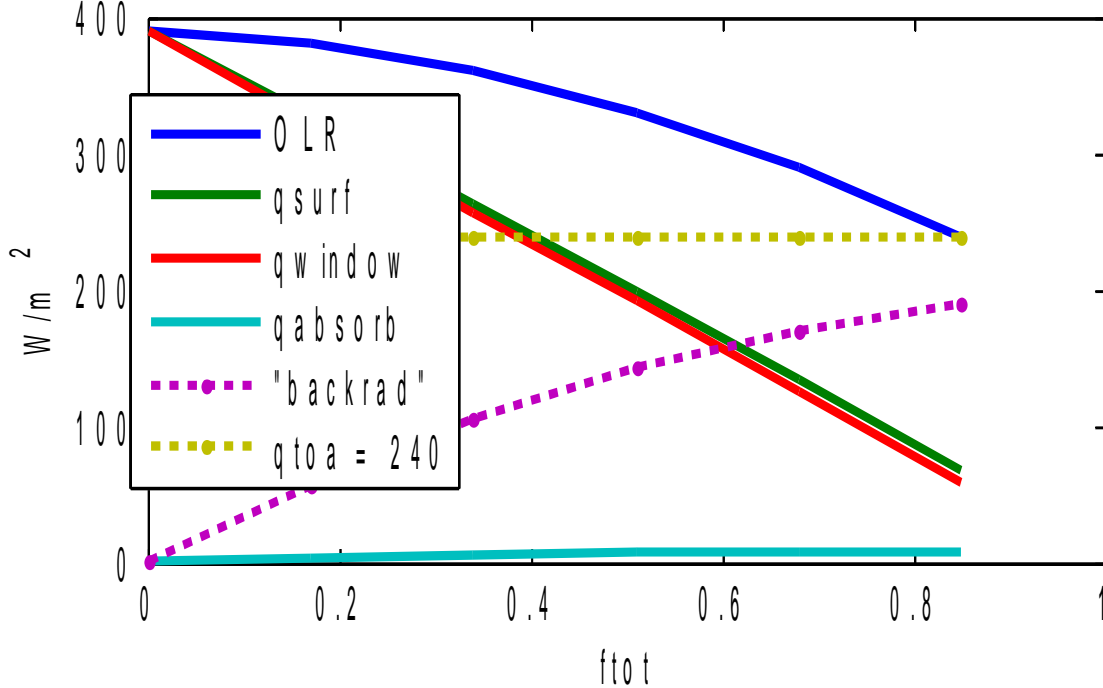
The red numbers are multiplied with 240 to obtain in Table A1 real FM fluxes in W/m^2 for a comparison with the corresponding numbers of the global energy budget of the stack model.

In figure A2 the results of the main equation of the one-stream stack model are represented. The equilibrium point is for $ftot = 0.849$:

OLR =240, LW surface flux =67 of which 59 through the window and 8 absorbed by the atmosphere.

Figure A2

fig 5.1 Main result of stack model
 $w = 1$ Planck = 4 nodes = 60 m = 7 height = 30 km LR = -6.5 K/km TsK = 2
 "backrad" is not backradiation of heat
 OLR, q_{surf} , q_{window} and q_{absorb} as function of f_{tot}



The curve “back-rad” is dotted, it are numbers which in the one-stream formulation appear in algebraic expressions with a negative sign. They do not have a physical meaning, they do not represent heat flow from cold to warm. See [1 , 2]

Table A1 fluxes

		fig A1	W/m^2		figA2	W/m^2
			FM		stack + FM	
Outgoing LW Radiation	OLR	(1)	240	calculated	240	
Incoming SW at TOA	FA	(1)	240	imposed	240	
Flux through window	ST	(1/4)	60		59	
Atmospheric Absorption	AA	(5/4)	300		8	
Back-radiation	ED	(5/4)	300		0	
SW absorption in atmosphere	F	(1/4)	60		60	
SW absorption in surface	FA-F	(3/4)	180		180	
LW surface flux	SU	(3/2)	360		67	
Convection	K	(1/2)	120		113 = 180 - 67	

In **Table A1** the results of FM are compared with those of the stack model, without the back-radiation and without the huge LW surface flux, typical for the two-stream formulation of Schwarzschild.

In **figure A3** is given the global and annual mean heat budget obtained with the stack model and with the experimental data according to FM from **figure A1** and **table A1**. Apart from the back-radiation and the Prevost type of LW surface flux in the FM data (both huge values 300), there is a difference in the convection term, 120 for FM and 113 for the stack model which. In the stack model, the number 113 for convection follows from the difference of incoming SW heat absorbed by the surface and the outgoing LW surface flux, presented in the last three lines of **table A1**.

**Figure A3 Global and annual mean heat budget in W/m^2 .
Stack Model with Miskolczi data, but without back-radiation.**

